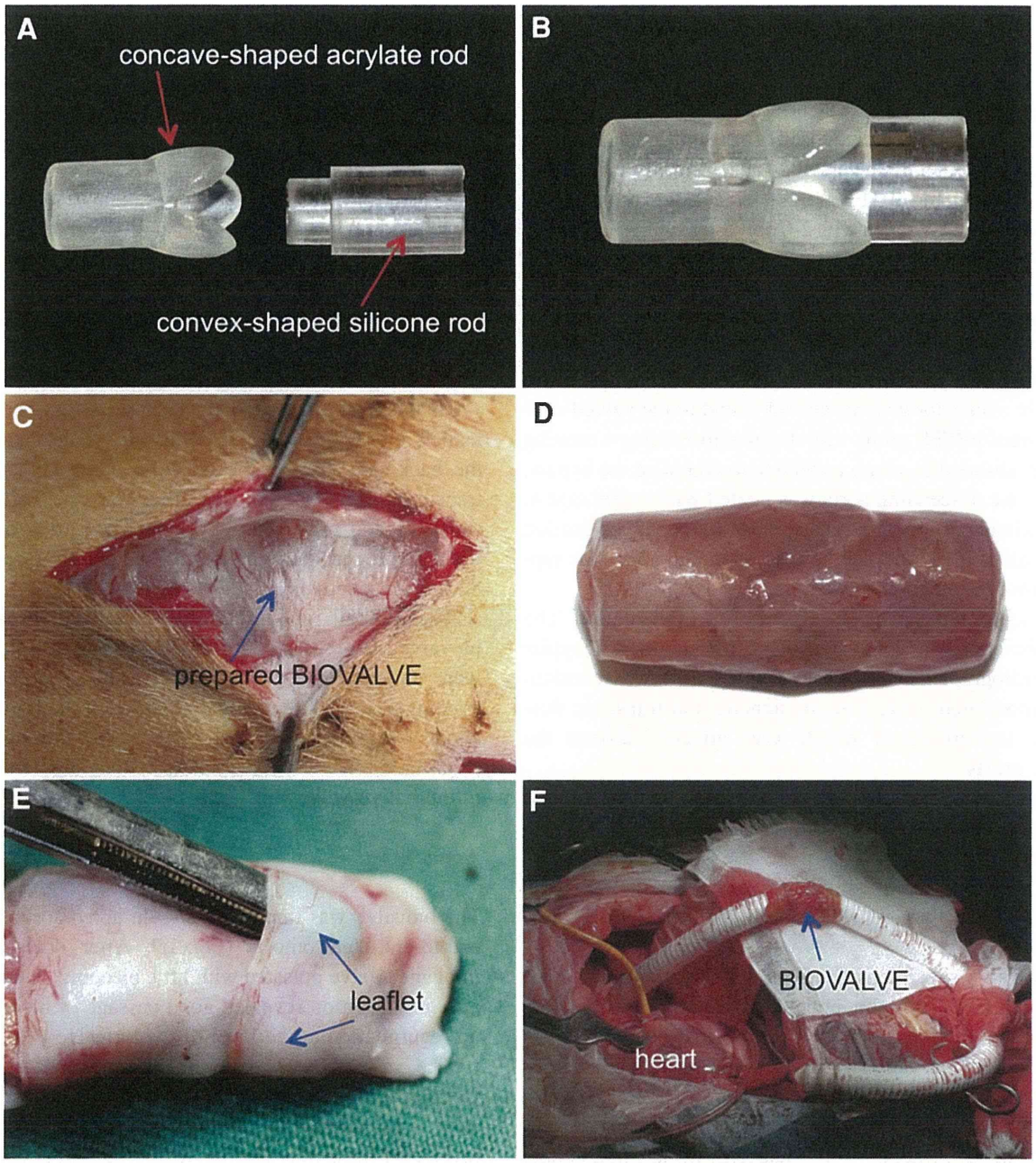

Fig. 1 Specially designed mold for the biovalve (**b**) assembled from a concave-shaped acrylate rod and a convex-shaped silicone rod (**a**) with a small 0.5-mm aperture for the formation of the leaflets. The concave-shaped rod contains three removable projections resembling the protrusions of the sinus of Valsalva. The molds were embedded for 2 months in a dorsal subcutaneous pouch in a goat. **c** After 8 weeks of implantation, the mold was encapsulated by connective tissue to form the biovalve (**d**). After removing the molds from each end of the implant, three thin leaflets were observed in the luminal side of the conduit. **e** Macroscopic observation of the formed leaflets after inversion of the biovalve conduit. **f** The biovalve was implanted between the apical portion of the left ventricle and descending aorta with interposition of ePTFE grafts without the use of cardiopulmonary bypass

In vivo evaluation of biovalves in the systemic circulation

To evaluate the biovalve under systemic circulation, we conducted an apico-aortic bypass with interposition of vascular grafts in the goat. Anesthesia was induced with 10 mg/kg of ketamine and maintained with 1–3 % isoflurane. The heart was exposed through a left thoracotomy at the fifth subcostal region. A valved conduit was composed of 14-mm ringed expanded polytetrafluoroethylene (ePTFE) grafts (GORE-TEX, W.L. Gore & Associates, Inc., Newark, DE). After treatment with a 1 % saline solution of water-soluble argatroban, a biovalve was sewed end to end to the ringed ePTFE grafts at both ends using a running 5-0 non-absorbable

suturing technique. The distal end of the valved conduit (ringed ePTFE grafts with the biovalve) was sewed end to side to the descending aorta using a partial occluding clamp and a running 4-0 non-absorbable suturing technique. An apical left ventricle connector was composed of a custom-made stainless steel conduit (outer diameters of 20 and 14 mm at either end) and a 14-mm ringed ePTFE graft. A felt cuff was sewed to the left ventricular (LV) apex with 2-0 polyester sutures with a felt strip. After injection of heparin sodium (200 U/kg), the LV apex was cored with a 19-mm custom-made ventricular coring device. Then, the apical left ventricle connector was inserted through the felt cuff into the LV apex without cardiopulmonary bypass and tied on the felt cuff. The apical left ventricle connector was sewed end to end to the valved conduit (ringed ePTFE grafts with the biovalve) using a running 4-0 non-absorbable suture technique to complete the bypass. Finally, the descending aorta was ligated with vessel tape at the proximal portion of the anastomosis of the valved conduit so that all of the blood flow to the abdominal aorta was supplied from the apico-aortic bypass.

An angiography was performed after implantation. The valve function was evaluated using transthoracic Doppler echocardiography every week. Bypass flow was continuously monitored using electromagnetic and transonic flow meters, the probes of which were attached around the ePTFE grafts.

Postoperative systemic anticoagulation for the ePTFE grafts was maintained with oral administration of warfarin sodium and aspirin.

Histological evaluation

The biovalve specimens acquired after implantation were fixed with 10 % formalin, embedded in paraffin, sliced into longitudinal sections, and finally stained with hematoxylin-eosin or Elastica van Gieson. In addition, a few sections of biovalve were also stained for α-smooth muscle actin (α-SMA) and factor VIII by immunohistochemical techniques; these proteins were detected using monoclonal antibodies (Dako Japan, Kyoto, Japan).

Statistics

Quantitative data were represented as mean ± standard deviation.

Results

Preparation and properties of biovalves

The assembled molds (Fig. 1b) embedded in the subcutaneous pouches of a goat for 2 months showed complete encapsulation with the connective tissue and marked neovascularization (Fig. 1c). The implants were easily harvested because only very fragile, irregular, and redundant tissues connected the developed biovalves and surrounding subcutaneous tissues, which could be dissected easily (Fig. 1d). The convex and concave rods were smoothly removed from each end of the implant because there was no adhesion between the molds and biovalves. The conduit had three protrusions, which were formed because of the shape of the concave substrate, resembling the sinus of Valsalva. A membranous tissue in the shape of a trileaflet was formed at the aperture of the combined rods, as intended by its design (Fig. 1e).

Analysis of the video data showed that the biovalve leaflets closed rapidly and tightly in synchronization with the backward flow in the diastolic phase (Fig. 2). In the transition phase of the flow direction, the valve opened smoothly and fully without flapping or hitting the conduit wall. The regurgitation ratio and orifice ratio were 12.0 and 82.7 %, respectively.

The strength and modulus of the leaflet part of the biovalve were 830 ± 270 and 1083 ± 289 kPa, which were almost equal to the native values, whereas in the conduit part, the strength and modulus of the biovalve were about five times larger than those of the native aorta (Fig. 3a, c). The biovalve had excellent suppleness similar to the native valve (Fig. 3b).

Application

The biovalve was implanted into an apico-aortic bypass by end-to-end anastomosis (Fig. 1f). After declamping, the implanted valve pulsated with little bleeding. An angiograph after implantation revealed good passage of blood flow and no regurgitation at the level of the biovalve (Fig. 4).

The valve function was evaluated using transthoracic Doppler echocardiography every week. Up to 2 months after implantation, echocardiographic examination revealed protrusions similar to the sinus of Valsalva and rapid opening (Fig. 5a) and closing (Fig. 5b) of the leaflets, and Doppler echocardiography (Fig. 5c) did not yield substantial evidence of stenosis and regurgitation.

The bypass flow by the electromagnetic flow meter was 2.6 ± 1.1 l/min throughout the experiment. A graph of flow waveform almost 2 months after implantation was presented in Fig. 6. The waveform has been maintained compared to pre-implanted pulsatile flow waveforms in Fig. 2.

In the 2 months after implantation, the goat was euthanized, and the biovalve implants were harvested. Macroscopic observation revealed that the shape and size of the leaflets were well maintained compared to those of native heart valve leaflets.

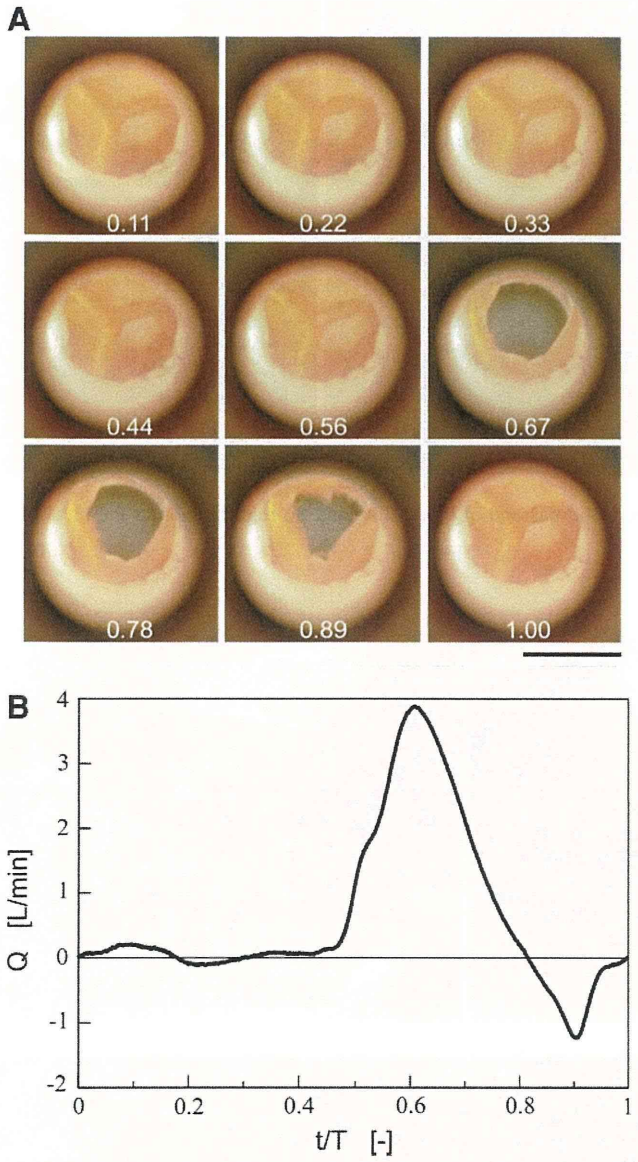

Fig. 2 **a** Valve movement under pulsatile conditions in one cycle ($T = 0.97$ s). The pulsatile rate was 62 bpm, and the average flow rate was 627 ml/min. The numbers in the photos are time/T. *Bar* 10 mm. **b** Pulsatile flow waveforms in one cycle

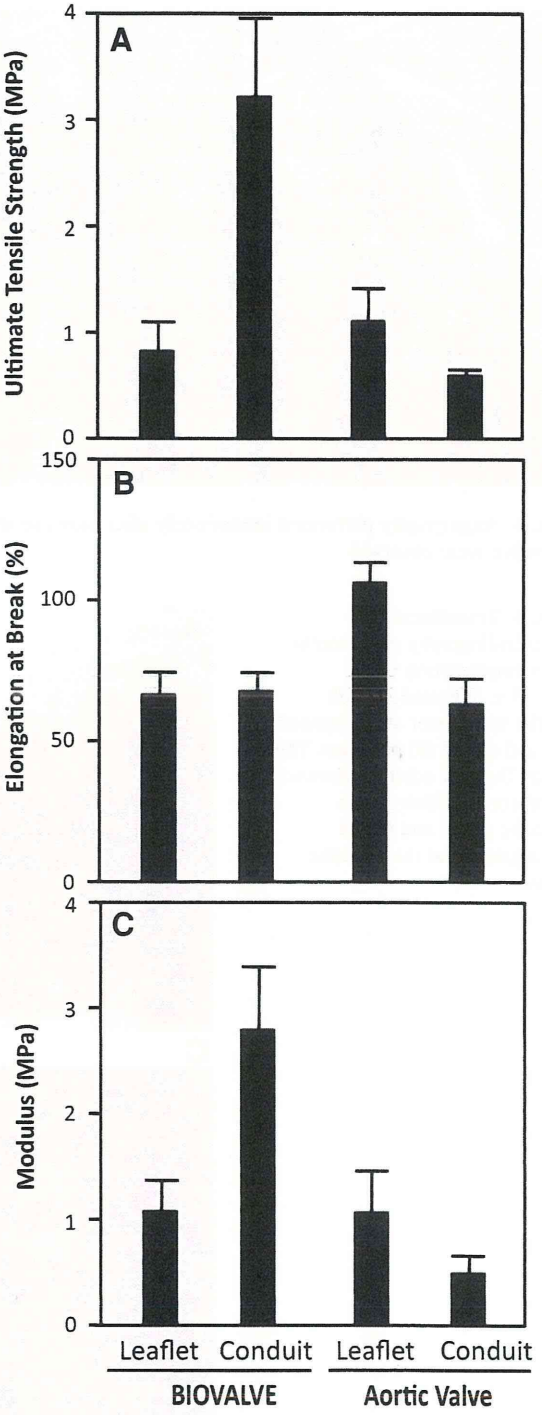

Fig. 3 Comparison of mechanical properties between biovalves and goat aortic valves. **a** The ultimate tensile strength, indicative of tissue strength, and **b** elongation at the break, indicative of tissue extensibility, were obtained from the stress-strain curves. **c** The modulus, indicative of tissue stiffness, was calculated as the slope of the linear part of the stress-strain curves. The error bars represent mean ± standard deviation ($n = 9$)

Histological evaluation

The whole body of the biovalve before implantation, including the valve leaflets and conduit, was mainly composed of collagen-rich tissue with fibroblasts (Fig. 7a). There were few elastic fiber and vascular cells. After implantation, wall thickness at the conduit and sinus of Valsalva significantly increased without any stenosis of the conduit (Fig. 5b), whereas leaflet thinness was well maintained (Fig. 7b). The conduit possessed a large amount of neovascularization (Fig. 7c). At the sinus, a thick elastic fiber formed although the main extracellular component was still collagen (Fig. 7d). Predominant cell types observed at the medial layer of the entire conduit walls included α-SMA positive, smooth muscle cells, and

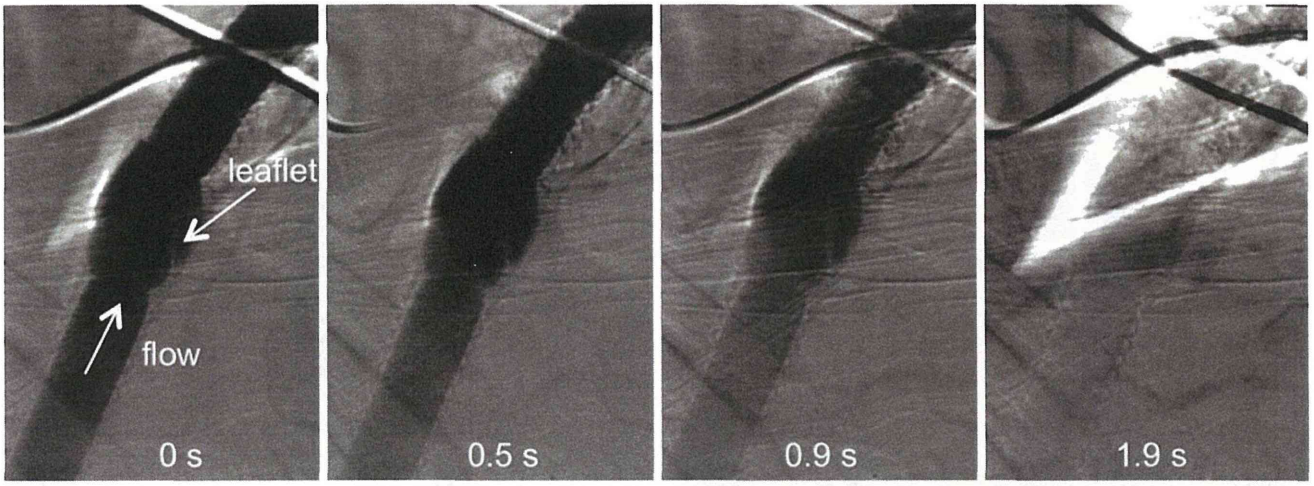

Fig. 4 Angiography performed immediately after biovalve implantation. Good passage of blood flow and no regurgitation at the level of the biovalve were observed

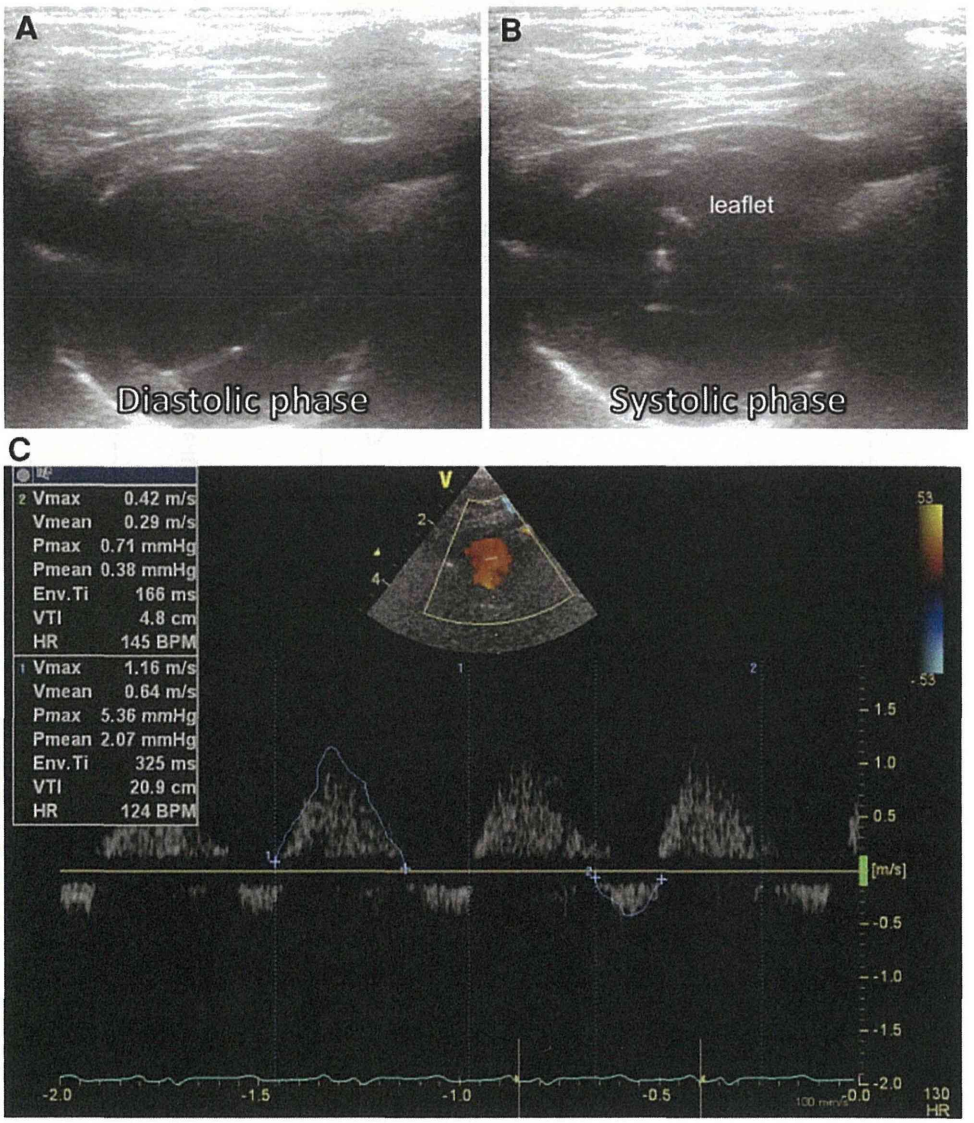

Fig. 5 Transthoracic echocardiography at 2 months after implantation of the biovalve indicated smooth leaflet movement at the opened (**a**) and closed (**b**) positions. The color Doppler echo (**c**) showed good forward flow at the systolic phase and trivial regurgitation at the diastolic phase

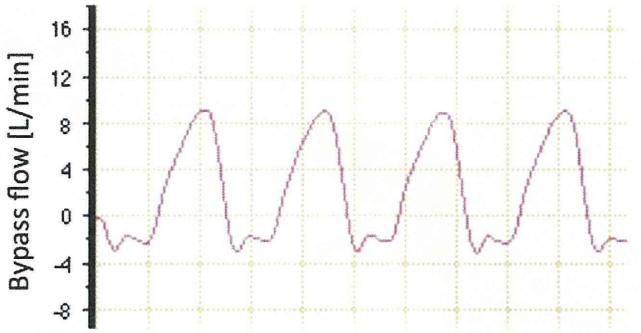

Fig. 6 A graph of flow waveform by the electromagnetic flow meter almost 2 months after implantation. The valve function has been almost maintained for 2 months

myofibroblasts (Fig. 7e–g) migrating toward the tip of the leaflet (Fig. 7h). Although the luminal surface was not covered with endothelial cells yet, no thrombus formation was observed on the smooth pseudointima (Fig. 7e, f).

Discussion

Biovalves were implanted into the systemic circulation as a pilot study with a limited experiment number and follow-up time in a goat model, although the sheep model is accepted by the FDA or other agencies as the most favorable model with regard to biodegradation/calcification. However, this is the first study reporting successful implantation of completely autologous tissue-valved conduits with no artificial support materials to the systemic circulation as aortic valves.

Due to the enormous number of patients suffering from aortic valve diseases, constructing aortic TEHVs has been the major study focus of many research groups. However, one of the predominant limitations for the development of an aortic TEHV is the use of an appropriate animal model for testing in the physiologically systemic circulation. Even in large animals, the anatomical implantation of the aortic valve conduit requires complex procedures such as cardiopulmonary bypass (CPB) and coronary arterial reconstruction. Therefore, in many previous studies, the prosthetic valves were implanted in the descending aorta [15, 16], where the pressure and flow pattern were completely different from the outflow of the left ventricle. Since implanted valves do not usually close tightly enough in this condition, valvular degeneration is often promoted. For this reason, our in vivo evaluation of biovalves in the systemic circulation with an apico-aortic bypass is worth reporting. Others have implanted the aortic valve in the pulmonary position, thus excluding the influence of systemic pressure on the implanted grafts from the beginning [17]. We have already reported successful implantation of the biovalves to the pulmonary valve position under CPB in a beagle model [13]. In a low-pressure condition, the biovalves functioned as pulmonary valves for 3 months with valvular tissue reconstruction. In this study, a potential of the biovalve as an aortic TEHV has been further increased.

The evaluation of valve function in vitro was performed under the pulsatile condition of 62 bpm with a flow rate of 627 ml/min. The condition was set for the implantation to goats weighing of about 40–50 kg, in which the average cardiac outflow is about 3.2–4.0 l/min (measured bypass flow: 2.6 ± 1.1 l/min) at a heart rate of 70–90 bpm. In the pulsatile flow circuit model, saline solution was selected as a working fluid for prevention of injury in biovalves made of natural tissues. The kinetic viscosity of blood is 4.44×10^{-6} m^2/s, which is about four times more than that of saline solution (1.00×10^{-6} m^2/s). Therefore, the flow condition in the circuit between the two different fluids, which is defined by the Reynolds number and Womersley number, needed to be adjusted for the evaluation of valve function using saline solution. The pulsatile rate and the flow rate calculated by the two numbers were 17.5–22.5 bpm and 800–1,000 ml/min (650 ± 275 l/min at the bypass), respectively.

Our biovalves were able to withstand systemic pressures without suffering structural or functional deterioration for as long as 2 months. The robust and elastic properties were obtained by slight treatment with diluted glutaraldehyde, which has been used clinically in porcine aortic valve or aortic valve repair. By designing a novel mold that reorganized biovalve construction, we developed the type VI biovalve, which demonstrates nearly perfect valve function. The key difference between the type V and VI molds is the aperture shape for leaflet formation. By preparing the valve leaflets in the open form, less regurgitation and an increase in the orifice ratio were observed upon in vitro examination. Furthermore, little regurgitation and no significant stenosis were confirmed during the observation period.

Since the biovalve was isolated from the heart and vascular tissues by ePTFE grafts in this model, α-SMA-positive cells that appeared in the conduit wall might have migrated from the surrounding connective tissue or could have originated from the fibroblasts existing in the biovalve wall since they were implanted. Further study is necessary to investigate their origin.

Regarding biovalve preparation for implantation, we followed the method of treatment with glutaraldehyde described by Duran et al. [18–22] for an aortic valve repair using an autologous pericardium leaflet. They explained that treated pericardium is used to increase the height of native aortic valve leaflets and commissures resulting in an increase in the coaptation zone. Glutaraldehyde treatment can provide more resistance against retraction and

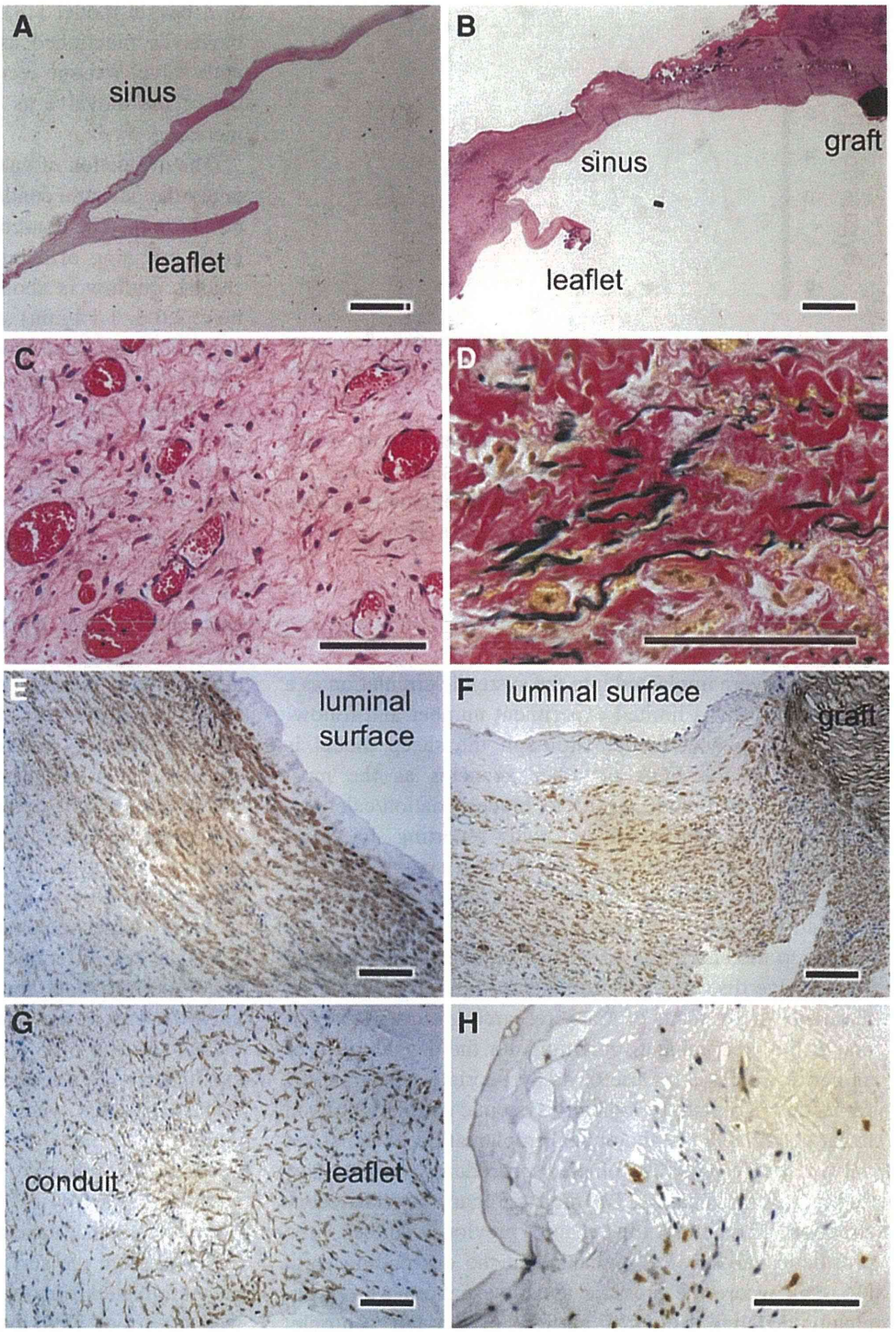

Fig. 7 Longitudinal sections of biovalve tissue before (**a**) and after (**b**) implantation (hematoxylin and eosin stain, *bar* 2 mm). **c** Neovascularization at the implanted biovalve conduit (hematoxylin and eosin stain, *bar* 100 μm). **d** Elastica van Gieson staining revealed a *black-colored* thick elastic fiber in the sinus region (*bar* 100 μm). Immunohistological staining for α-SMA revealed that predominant smooth muscle cells or myofibroblasts were observed at the sinus region (**e**), the proximal anastomosis region (**f**), and base (**g**) and tip (**h**) of the leaflet (*bar* 100 μm)

degeneration and maintain the intrinsic tissue pliability of the pericardium. However, treatment with glutaraldehyde may destroy native cells and cause denaturation of connective tissue even though the immersion is at a low dose and for a short time. Further examination is needed to determine the optimal method for biovalve preparation.

At 2 months after implantation, there were few endothelial cells at the luminal surface, whereas no thrombus formation was observed. Implantation of the biovalve at the aortic root or directly anastomosed to the native aorta was expected to result in the rapid migration of both endothelial and mesenchymal cells from the anastomotic sites, leading to quick tissue organization and maturation. This was observed in the anatomically implanted beagle model. Further implantation experiments with longer observational periods are ongoing.

Conclusion

Completely autologous type VI biovalves with robust and elastic characteristics appropriate for aortic valve replacement were developed by in-body tissue architecture technology using an improved mold design. Slight glutaraldehyde treatment enabled the type VI biovalve to achieve desirable idealistic mechanical properties for aortic valve replacement with respect to both valvular function and surgical handling. The biovalves withstood systemic pressure without unexpected dilatation or aneurysm formation in the conduit portion and degeneration or sclerosis of the valvular leaflet, which could be responsible for aortic valve regurgitation or stenosis within 2 months of implantation. Rapid tissue maturation with elastic fiber formation and the predominant appearance of α-SMA-positive cells in the completely autologous tissue without synthetic support materials might induce the growth potential of the valves.

Acknowledgments The authors thank Ms. Manami Sone, Mr. Yuji Shimakawa, and Dr. Yue-Min Zhou for their participation in this study. This study was funded in part by a Grant-in-Aid for Scientific Research (B19390368, B21360123) from the Ministry of Education, Culture, Sports, Science and Technology of Japan.

References

1. Cosgrove DM, Lytle BW, Taylor PC, Camacho MT, Stewart RW, McCarthy PM, Miller DP, Piedmonte MR, Loop FD. The Carpentier-Edwards pericardial aortic valve. Ten-year results. J Thorac Cardiovasc Surg. 1995;110:651–62.
2. Shin'oka T, Ma PX, Shum-Tim D, Breuer CK, Cusick RA, Zund G, Langer R, Vacanti JP, Mayer JE. Tissue-engineered heart valves. Autologous valve leaflet replacement study in a lamb model. Circulation. 1996;94:164–8.
3. Dohmen PM, Ozaki S, Nitsch R, Yperman J, Flameng W, Konertz W. A tissue engineered heart valve implanted in a juvenile sheep model. Med Sci Monit. 2003;9:97–104.
4. Vesely I. Heart valve tissue engineering. Circ Res. 2005;97:743–55.
5. Baraki H, Tudorache I, Braun M, Höffler K, Görler A, Lichtenberg A, Bara C, Calistru A, Brandes G, Hewicker-Trautwein M, Hilfiker A, Haverich A, Cebotari S. Orthotopic replacement of the aortic valve with decellularized allograft in a sheep model. Biomaterials. 2009;30:6240–6.
6. Nakayama Y, Ishibashi-Ueda H, Takamizawa K. In vivo tissue-engineered small-caliber arterial graft prosthesis consisting of autologous tissue (biotube). Cell Transplant. 2004;13:439–49.
7. Watanabe T, Kanda K, Ishibashi-Ueda H, Yaku H, Nakayama Y. Development of biotube vascular grafts incorporating cuffs for easy implantation. J Artif Organs. 2007;10:10–5.
8. Sakai O, Kanda K, Ishibashi-Ueda H, Takamizawa K, Ametani A, Yaku H, Nakayama Y. Development of the wing-attached rod for acceleration of "Biotube" vascular grafts fabrication. J Biomed Mater Res B Appl Biomater. 2007;83:240–7.
9. Watanabe T, Kanda K, Ishibashi-Ueda H, Yaku H, Nakayama Y. Autologous small-caliber "Biotube" vascular grafts with argatroban loading: a histomorphological examination after implantation to rabbits. J Biomed Mater Res B Appl Biomater. 2010;92:236–42.
10. Hayashida K, Kanda K, Yaku H, Ando J, Nakayama Y. Development of an in vivo tissue-engineered, autologous heart valve (the biovalve): preparation of a prototype model. J Thorac Cardiovasc Surg. 2007;134:152–9.
11. Hayashida K, Kanda K, Oie T, Okamoto Y, Ishibashi-Ueda H, Onoyama M, Tajikawa T, Ohba K, Yaku H, Nakayama Y. Architecture of an in vivo-tissue engineered autologous conduit "Biovalve". J Biomed Mater Res B Appl Biomater. 2008;86:1–8.
12. Nakayama Y, Yamanami M, Yahata Y, Tajikawa T, Ohba K, Watanabe T, Kanda K, Yaku H. Preparation of a completely autologous trileaflet valve-shaped construct by in-body tissue architecture technology. J Biomed Mater Res B Appl Biomater. 2009;91:813–8.
13. Yamanami M, Yahata Y, Uechi M, Fujiwara M, Ishibashi-Ueda H, Kanda K, Watanabe T, Tajikawa T, Ohba K, Yaku H, Nakayama Y. Development of a completely autologous valved conduit with the sinus of valsalva using in-body tissue architecture technology: a pilot study in pulmonary valve replacement in a beagle model. Circulation. 2010;122:S100–6.
14. Nakayama Y, Yahata Y, Yamanami M, Tajikawa T, Ohba K, Kanda K, Yaku H. A completely autologous valved conduit prepared in the open form of trileaflet (type VI biovalve): mold design and valve function in vitro. J Biomed Mater Res Part B Appl Biomater. 2011;99B:135–41.
15. Conconi MT, Rocco F, Spinazzi R, Tommasini M, Valfrè C, Busetto R, Polesel E, Albertin G, Dei Tos A, Iacopetti I, Cecchetto A, Zussa C, Grigioni M, Parnigotto PP, Nussdorfer GG. Biological fate of tissue-engineered porcine valvular conduits xenotransplanted in the sheep thoracic aorta. Int J Mol Med. 2004;14:1043–8.
16. Gulbins H, Pritisanac A, Pieper K, Goldemund A, Meiser BM, Reichart B, Daebritz S. Successful endothelialization of porcine glutaraldehyde-fixed aortic valves in a heterotopic sheep model. Ann Thorac Surg. 2006;81:1472–9.
17. Van Nooten G, Somers P, Cornelissen M, Bouchez S, Gasthuys F, Cox E, Sparks L, Narine K. Acellilar porcine and kangaroo aortic valve scaffolds show more intense immune-mediated calcification than cross-linked Toronto SPV valves in the sheep model. Interact Cardiovasc Thorac Surg. 2006;5:544–9.
18. Duran CMG, Alonso J, Gaite L, Alonso C, Cagigas JC, Marce L, Fleitas MG, Revuelta JM. Long-term results of conservative repair of rheumatic aortic valve insufficiency. Eur J Cardiothorac Surg. 1988;2:217–23.
19. Duran CM, Gometza B, Kuma N, Gallo R, Bjonastad K. From aortic cusp extension to valve replacement with stentless pericardium. Ann Thorac Surg. 1995;60:S428–32.
20. Duran CMG, Gometza B, Kuma N. Aortic valve replacement with freehand autologous pericardium. J Thorac Cardiovasc Surg. 1995;110:511–6.
21. Duran C, Gometza B, Kuma N, Gallo R, Bjonastad K. Treated bovine and autologous pericardium: surgical technique. J Cardiac Surg. 1995;10:1–9.
22. Ozaki S, Kawase I, Yamashita H, Uchida S, Nozawa Y, Matsuyama T, Takatoh M, Hagiwara S. Aortic valve reconstruction using self-developed aortic valve plasty system in aortic valve disease. Interact Cardiovasc Thorac Surg. 2011;12:550–3.

Polymer Degradation and Stability 98 (2013) 958–962

Contents lists available at SciVerse ScienceDirect

Polymer Degradation and Stability

journal homepage: www.elsevier.com/locate/polydegstab

Polyethylene glycol-solvolyzed poly-(L)-lactic acids and their stereocomplexes with poly-(D)-lactic acid

Hisanori Ando [a,*], Maki Oshima [b], Yasuhide Nakayama [c], Atsuyoshi Nakayama [b]

[a] Research Institute for Ubiquitous Energy Devices, National Institute of Advanced Industrial Science and Technology (AIST), 1-8-31 Midorigaoka, Ikeda, Osaka 563-8577, Japan
[b] Health Research Institute, AIST, 1-8-31 Midorigaoka, Ikeda, Osaka 563-8577, Japan
[c] Division of Medical Engineering and Materials, National Cerebral and Cardiovascular Center Research Institute, 5-7-1 Fujishiro-dai, Suita, Osaka 565-8565, Japan

ARTICLE INFO

Article history:
Received 9 October 2012
Received in revised form
18 February 2013
Accepted 25 February 2013
Available online 5 March 2013

Keywords:
Polylactic acid
Stereocomplex
Solvolysis
Polyethylene glycol
Contact angle
Biodegradation

ABSTRACT

Poly-(L)-lactic acid (PLLA) was solvolyzed with polyethylene glycol (PEG) with different ratios of PLLA and PEG under dry conditions. The obtained materials were found to be the block copolymer of PLLA and PEG (PLLA/PEG) from NMR analysis of which the number average molecular weights ranged from 6×10^3 to 2×10^4 g mol^{-1}. The films of stereocomplex (SC) of PLLA/PEG and poly-(D)-lactic acid (PDLA) were prepared by solvent casting method, and the thermal properties and the contact angle of the films were examined. The melting temperatures of PLLA/PEG and the corresponding SC with PDLA linearly decreased with the increase in the PEG content from 110 to 170 °C. The contact angle of PLLA/PEG became lower when the PEG content in the PLLA/PEG was higher, while their SCs with PDLA showed no clear correlation with the PEG content. Biodegradability of PLLA/PEGs and their SCs were also investigated with respect to the EG content.

1. Introduction

The development of bioplastics, which can be produced from renewable resources, is one of the most important research topics in the "carbon neutral concept", and thus varieties of research have been carried out so far [1]. Among the bioplastics, polylactic acid (PLA) is expected to be replaced with conventional thermoplastic polymers produced from petroleum resources because it shows excellent thermal and mechanical properties. However, it has some drawbacks, such as thermal stability, biodegradability and hydrophobicity, and these may be obstacles to the spreading of PLA.

Stereocomplex (SC) of PLA, firstly reported by Ikada et al., is a polymer blend obtained by mixing equimolar of poly-(L)-lactic acid (PLLA) and poly-(D)-lactic acid (PDLA) [2]. The SC has preferable properties compared with the homopolymers of PLA, such as high melting temperature, improved tensile strength, and high transparency [3–5]. Kimura et al. developed new block copolymers of PLLA and PDLA (stereoblock polylactic acids, sb-PLA), which effectively form SC with a molecular weight higher than 100 kDa [6].

We have previously synthesized L-lactide/glycidol copolymers at various compositions and reported that the thermal properties and biodegradability of the material are controllable simply by changing the comonomer feed ratio [7].

In the present study, we solvolyzed PLLA with PEG to produce the block copolymer of PLLA and PEG (PLLA/PEG) with various feed ratios and prepared its SC with PDLA to alter the hydrophilicity and biodegradability. Polyethylene glycol is a hydrophilic polymer having hydroxy groups at both ends which can react with the ester groups in PLA to give AB- and ABA-type block copolymers of PLA and PEG (see Scheme 1). The effects of PEG segment to the SCs on the thermal property, hydrophilicity and biodegradability are discussed on the basis of the results of the DSC, NMR, contact angle measurements and enzymatic hydrolysis using proteinase K.

2. Experimental

2.1. Materials

PLLA (Laclier®, pellet) was supplied by Fuji Chemical. (D)-Lactide (PURASORB® D) and PEG with an average molar mass of 1000 were obtained from Purac Biochem and Sigma–Aldrich, respectively. Tetraphenyl tin (IV) and Proteinase K were purchased from Wako Pure Chemical Industries. All chemicals and solvents were of

* Corresponding author. Tel.: +81 72 751 9182; fax: +81 72 751 9629.
E-mail address: h-ando@aist.go.jp (H. Ando).

0141-3910/$ – see front matter © 2013 Elsevier Ltd. All rights reserved.
http://dx.doi.org/10.1016/j.polymdegradstab.2013.02.016

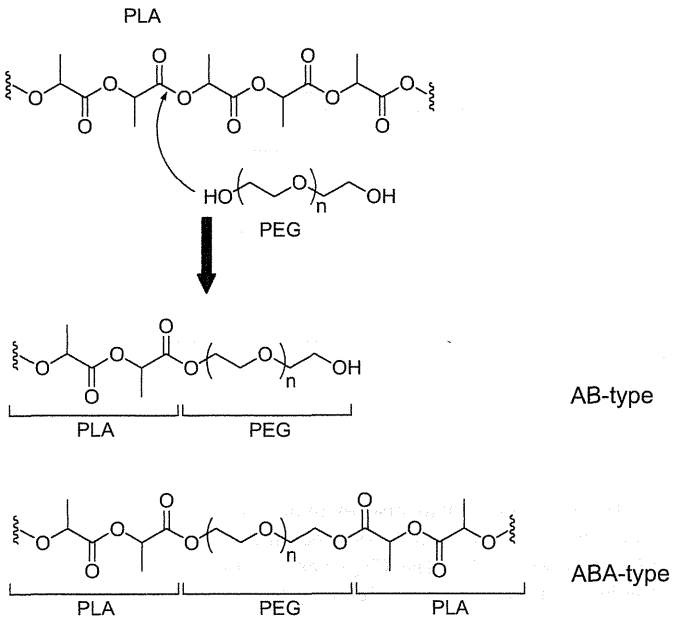

Scheme 1. Solvolysis of PLA with PEG.

special grade where obtainable and were used without further purification.

2.2. Synthesis of PDLA

(D)-Lactide (14.4 g, 100 mmol) was placed in a round-bottom flask (100 mL) equipped with a condenser and a desiccant tube. Tetraphenyl tin (IV) (0.13 g, 0.3 mmol) was added as solid, then the mixture was heated to 150 °C with stirring. The mixture became a pale yellowish solid after 8 h and the temperature was kept at 150 °C for 2 days. After cooling to room temperature, the solid was dissolved in a minimum volume of chloroform. The chloroform solution was poured into methanol with stirring, giving a fibrous precipitate. The precipitate was washed with methanol twice and dried at 50 °C under reduced pressure.

2.3. Solvolysis of PLLA

To avoid the hydrolysis of PLLA by residual water in the glass wares, they were subjected to a careful drying procedure under dried N_2 gas at 100 °C for several hours before use. PLLA and PEG were placed in a round-bottom flask (50 mL) equipped with a condenser and a desiccant tube and were heated at 100 °C with stirring under reduced pressure for 3 h to remove water. The reaction was initiated by raising the temperature to 220 °C. After 16 h, the reaction mixture was cooled down to room temperature, yielding the crude product (brownish hard solid). The crude product was dissolved in a minimum amount of chloroform, then the solution was poured into methanol with stirring to give precipitates. The precipitates were collected and washed with methanol twice, followed by vacuum drying.

2.4. Preparation of films

The polymer films were prepared by solvent casting method from the chloroform solution of the materials (3 w/v%) for several days, subsequently followed by vacuum drying at 50 °C. The films of SCs were prepared by using the mixture of the same volume of the chloroform solutions (6 w/v%) of PLLA/PEG and PDLA. All films were dried at 50 °C under vacuum for several hours and stored in a desiccator.

2.5. Measurements

Gel permeation chromatography (GPC) was performed with HLC-8220GPC system (Tosoh, Japan) by using chloroform as eluant (0.6 mL min^{-1}) at 35 °C. Three columns, TSKgel $5000H_{xL}$, TSKgel $4000H_{xL}$ and TSKgel $3000H_{xL}$ (Tosoh), were connected successively in this order. The number-average molecular weight (M_n) and the weight-average molecular weight (M_w) of the materials were calculated from the retention time of the polystyrene standard samples.

The thermal properties of the materials were investigated by differential scanning calorimetry (DSC), using a DSC3100S (Bruker AXS K.K., Japan). All the scans were carried out from 30 to 300 °C at a heating rate of 10 °C min^{-1} under nitrogen atmosphere. Data for melting temperature (T_m) and the enthalpy of fusion (ΔH) were taken from the first heating scan.

^1H NMR spectra were recorded using a JNM-ECA-500 spectrometer (JEOL, Japan) (500 MHz for ^1H) at room temperature in $CDCl_3$ or D_2O with tetramethyl silane or sodium 3-(trimethylsilyl) propane-1-sulfonate as internal standards, respectively.

The static (equilibrium) contact angle of the films of PLLA/PEGs and their SCs with PDLA was measured with a Model-PGX (FIBRO System AB, Sweden) equipment. The samples for measuring the contact angle were deposited on the slide glass from 1 wt% chloroform solution of the material using simple spin coating at 3000 rpm for 35 s.

2.6. Enzymatic hydrolysis

The biological degradation of the materials was tested by the hydrolysis using Proteinase K in the 0.1 M phosphate buffer solution (NaH_2PO_4/Na_2HPO_4, pH = 7.0). The material (a piece of film, 20 mg) and the buffer solution of the enzyme (2 mL, 200 units) were placed in the test tube and heated at 37 °C for 48 h. After thermal denaturation of enzyme, the solution was filtrated with polytetrafluorethylene membrane (pore size, 0.2 μm) and water was removed in the drying oven at 60 °C. The deposited material was dissolved in D_2O for NMR analysis. The biodegradability was estimated from the integration of proton peaks of external standards of (L)-lactic acid and ethylene glycol. The data were corrected by subtracting both blank values; an enzyme blank level and a polymer blank level. The polymer blank level stands for standard nonenzymatic polymer hydrolyzability under the same conditions.

3. Results and discussion

3.1. PEG-solvolyzed PLLA

The properties of PLLA, PDLA and the PEG-solvolyzed PLLA (PLLA/PEG) are summarized in Table 1. The M_n values for the solvolyzed material ranged from 6.4×10^3 to 21×10^3 g mol^{-1}, depending on the PLLA/PEG feed ratio and reaction conditions. According to the M_w/M_n the solvolysis seems to proceed uniformly while the significant decrease of M_n and M_w was observed for all PLLA/PEGs compared with the original PLLA. The longer reaction time with higher temperature resulted in the product with extremely low M_n and M_w (runs 1 and 5).

As for ^1H NMR analysis, the peaks at δ1.58 ppm (doublet) and δ5.18 ppm (quartet) can be assigned to the methylene and methyl protons in $-O-CH(CH_3)-C(=O)-$ fragment (LA) and δ3.64 ppm (singlet) to the $-O-CH_2-CH_2-$ fragment (EG), where LA and EG represent the lactic acid unit and the ethylene glycol unit, as diad homo sequences (−LA−LA−, −EG−EG−), respectively. The weak

Table 1
Properties of PEG-solvolyzed PLLA under various reaction conditions.

Polymerization conditions					Physical/chemical properties of the materials								
Run	PLLA g(mmol)	PEG g (mmol)	Temp. (°C)	Time (h)	M_n ($\times 10^{-3}$)	M_w ($\times 10^{-3}$)	M_w/M_n	T_m (°C)	ΔH (kJ g^{-1})	EG cont. (%)[a]	Copolym. cont. (%)[b]	[$EG_{est.}$ cont.] (%)[c]	[$EG_{Theor.}$ cont.] (%)[d]
L	PLLA	–	–	–	92	127	1.4	162	43	–	–	–	–
D	PDLA	–	–	–	44	64	1.5	176	51	–	–	–	–
1	5 (0.05)	0.5 (0.5)	190	12	21	34	1.7	164	39	4.9	65	7.5	14
2	5 (0.05)	0.25 (0.25)	190	12	18	34	1.8	157	41	3.8	43	8.8	7.6
3	5 (0.05)	0.1 (0.1)	190	12	21	35	1.7	158	45	0.67	9	7.6	3.2
4	5 (0.05)	0.05 (0.05)	190	12	12	17	1.5	161	43	0.22	2	13	1.6
5	5 (0.05)	0.5 (0.5)	220	18	6.4	7.8	1.2	126	30	6.5	28	23	14
6	5 (0.05)	0.005 (0.005)	220	18	8.9	11	1.3	108	11	17	99	17	0.16

[a] Calculated from the peak intensity of ^{1}H NMR spectrum. The details are described in the text.
[b] Calculated from the ratio of EG cont. and $EG_{est.}$ cont.
[c] Calculated from the GPC result. The details are described in the text.
[d] Calculated from the feed ratio of PLLA and PEG.

peaks at δ4.32–4.22 ppm and δ3.75–3.67 ppm were also observed which can be assigned to the methylene protons in the hetero connecting fragment (–LA–EG–) and δ4.36 ppm(quartet) can be assigned as a methyne proton in an end group of LA. Observation of the hetero sequence means that the block copolymer is successfully produced (see Fig. 1). A block length of the PEG segment in run 1 was calculated from the intensity ratio of the protons of homo and hetero sequences. The value is ca. 25. The molecular weight of the repeating unit of PEG segment is 44, meaning that the molecular weight of PEG segment in the copolymer is ca. 1100. This is almost the same as the original molecular weight of PEG. The results show that a PLLA/PEG molecule contains one PEG segment in both AB-type and ABA-type block copolymers. The EG content (%) in PLLA/PEG was calculated from the peak intensity (I) according to equation (1), as the ^{1}H NMR signals from the terminal protons of PLLA and PEG are negligibly small compared with those from the main body.

$$\text{Obsd. EG cont.}(\%) = I_{[\delta 3.64]} / \left(I_{[\delta 1.58]} + I_{[\delta 5.18]} + I_{[\delta 3.64]} \right) \times 100 \quad (1)$$

The EG content was also estimated from the M_n obtained by GPC. The molecular weight of repeating unit of PLLA (–OCH(CH_3)CO–) and PEG (–O–CH_2–CH_2–) are 72 and 44, respectively, then the EG content can be calculated by the following equation:

$$\text{GPC Est. EG cont.}(\%) = U_{EG} / (U_{LA} + U_{EG}) \times 100 \quad (2)$$

where U_{EG} and U_{LA} are the number of the repeating units for EG and LA, respectively, and they can be calculated by the equations as follows when the molecular weight of PEG is 1000:

$$U_{EG} = 1000/44 = 22.7$$

$$U_{LA} = (M_n - 1000)/72$$

In comparison with the estimated EG content from GPC results, some observed EG contents are small. For example, the observed EG content (3.8%) was significantly low compared with that from GPC (8.8%, run 2). That is, LA content in the obtained polymer is larger than the estimated value from GPC, suggesting that the obtained

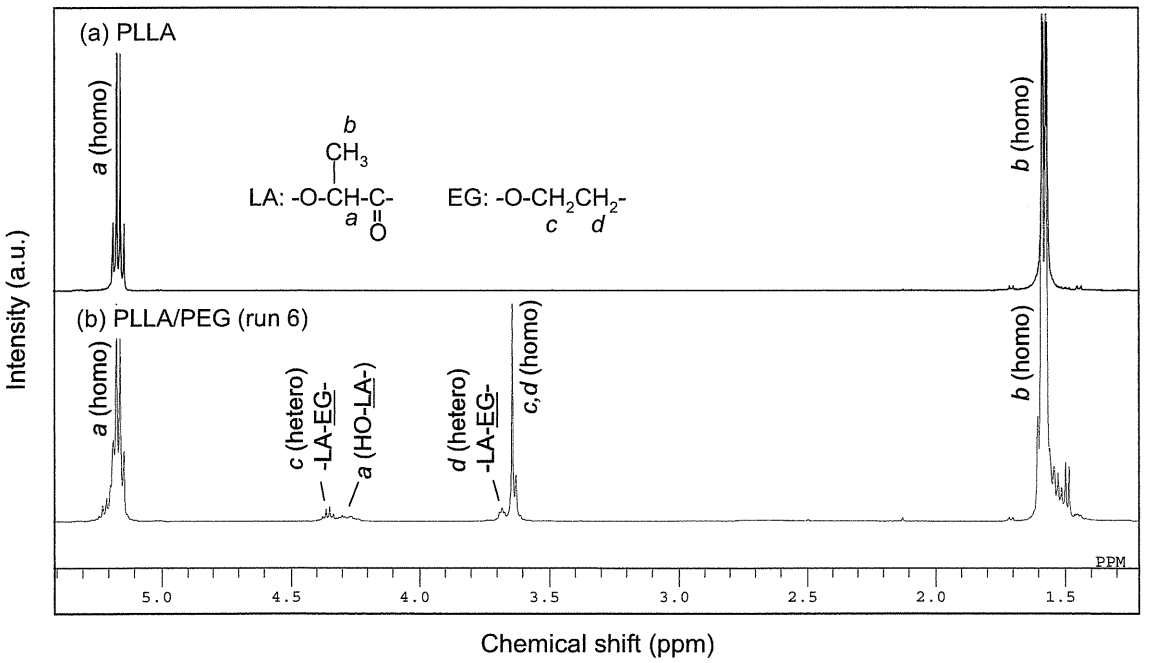

Fig. 1. ^{1}H NMR spectra of PLLA (a) and PLLA/PEG (run 6) (b).